

AUTOMATIC DIGITAL PRE-COMPENSATION IN IQ MODULATORS

J. Tuthill and A. Cantoni

Australian Telecommunications Research Institute
Curtin University of Technology
GPO Box U1987, Perth, WA, 6845, Australia

ABSTRACT

In digital IQ modulators generating Continuous Phase Frequency Shift Keying (CPFSK) signals, departures from flat-magnitude, linear phase in the pass bands of signal reconstruction filters in the I and Q channels cause ripple in the output signal envelope. Amplitude Modulation (AM) in the signal envelope function produces undesirable sidelobes in the FSK signal spectrum when the signal passes through nonlinear elements in the transmission path.

A structure is developed for digitally pre-compensating for the magnitude and phase characteristics of signal reconstruction filters. Optimum digital pre-compensation filters are found using least squares (LS) techniques and we propose a method by which the optimum pre-compensation filters can be estimated using test input signals. This method can be used as part of an automatic compensation process.

1. INTRODUCTION

CPFSK is an important technique for band-pass data transmission [1]. There are a number of methods for generating CPFSK signals and in this paper we consider the method of IQ (In-phase and Quadrature) modulation.

The IQ modulator structure is shown in Fig. 1. Here, the I and Q channel baseband signals are generated digitally and converted into analogue signals using D/A converters and signal reconstruction filters before modulation and transmission.

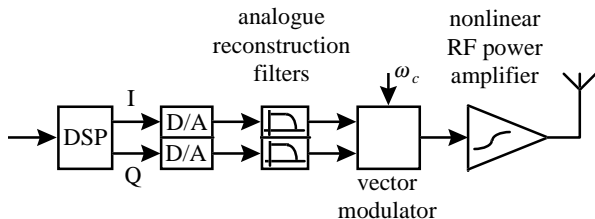


Figure 1. IQ modulation system.

Distortion terms in radio frequency (RF), nonlinear power amplifiers (PA's) (for radio channels of interest here) can be adequately described by amplitude-to-amplitude (AM-AM) and amplitude-to-phase (AM-PM) conversion characteristics [2] which are functions of the envelope of the amplifier input RF signal [3].

A important property of CPFSK signals is that they have constant envelope thus making these signals particularly useful for communication systems which employ RF PA's having nonlinear transfer characteristics. Imperfections in the implementation of the IQ modulator, however, result in the loss

of the desired constant envelope property. In this paper we are concerned only with imperfections in the reconstruction filters.

The signal reconstruction process produces distortion in the I and Q channel signals and introduces ripple into the vector modulator output signal envelope. This distortion is due to departures from a linear phase, constant magnitude frequency response in each reconstruction filter and gain and phase imbalances between these two filters.

Extensive work has been done on *pre-distortion* techniques to compensate for nonlinearities in power amplifiers, e.g. [4], however most of this work has ignored the effects of reconstruction filters. In [5] a study of the effects of reconstruction filters on pre-distortion PA linearisers was presented and in [6] a compensation method was presented to reduce the effects of gain and phase mismatch between reconstruction filters in a multichannel context.

In this paper we propose the use of digital signal *pre-shaping* filters in the I and Q channels to pre-compensate for *both* imbalances between the reconstruction filters *and* departures from constant magnitude, linear phase in the passband of each reconstruction filter. A digital pre-compensation structure is presented and the optimum pre-compensation filters are found using a least squares approach. A method is proposed by which the pre-compensation filters can be found automatically and simulation studies highlight the effectiveness of the method.

2. OPTIMUM DIGITAL PRE-COMPENSATION

The IQ modulator structure considered here is shown in Fig. 2.

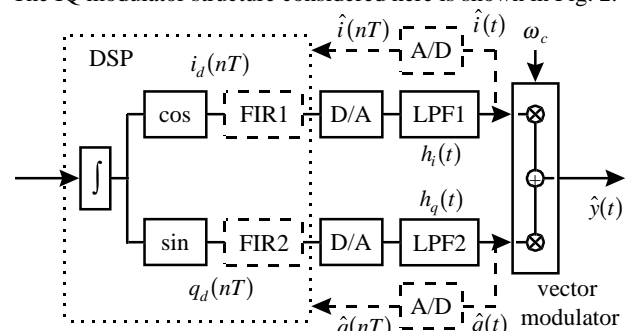


Figure 2. IQ modulator and pre-compensation structure.

The dashed boxes in Fig. 2 show the proposed digital pre-compensation structure. The FIR filters are designed to pre-shape the I and Q channel signals prior to passing through the D/A converters and reconstruction filters. The two sets of FIR filter weights are chosen such that the differences between the actual

channel response (from the FIR filter input to the output of the A/D) and a *desired channel response* is minimised according to some specified criterion. Since the actual analogue filters, $h_1(t)$ and $h_2(t)$, differ from each other, the impulse responses of FIR 1 and FIR 2 may also be different depending on the optimisation criterion used.

One channel (I or Q), from the input to the FIR pre-compensation filter to the output of the A/D converter is shown in the lower branch of Fig. 3. The upper branch represents the nominal desired system, i.e., the response that the I or Q channel is required to have. (We need only consider one channel as the same optimisation process will apply to the other, although a different pre-compensation filter will result since $h(t)$ will be different.)

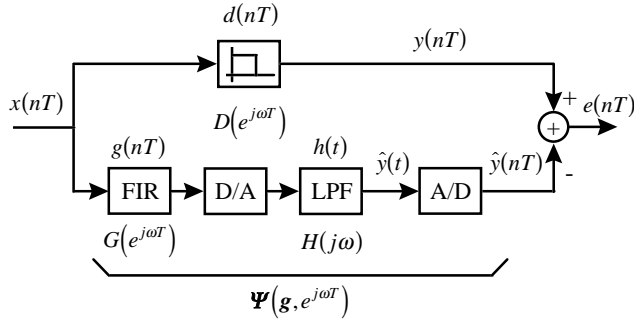


Figure 3. I or Q channel pre-compensation structure.

We define the cost function for the least-squares optimisation to be the integral of the magnitude-squared difference between the desired response, $D(e^{j\omega T})$, and the actual response, $\Psi(g, e^{j\omega T})$, over the frequency interval Ω :

$$J(\mathbf{g}) = \int_{\Omega} |D(e^{j\omega T}) - \Psi(\mathbf{g}, e^{j\omega T})|^2 d\omega, \quad (1)$$

where $\mathbf{g} \in R^{K \times 1}$ is the vector of FIR filter weights to be determined. The integrand in (1) is a periodic function in ω with period ω_s , where $f_s = \omega_s/2\pi$ is the system sampling frequency. The frequency interval in (1) is therefore chosen to be $\Omega = [-\omega_s/2, \omega_s/2]$.

Expanding the right hand side of (1) gives

$$J(\mathbf{g}) = c - 2\mathbf{g}^T \mathbf{p} + \mathbf{g}^T \mathbf{R} \mathbf{g} \quad (2)$$

where

$$c = \int_{\Omega} |D(e^{j\omega T})|^2 d\omega, \quad (3)$$

$$\mathbf{p} = \frac{1}{2} \left[\int_{\Omega} D(e^{j\omega T}) s^H(e^{j\omega T}) H_d^*(e^{j\omega T}) d\omega \right. \\ \left. \int_{\Omega} D^*(e^{j\omega T}) s^T(e^{j\omega T}) H_d(e^{j\omega T}) d\omega \right], \quad (4)$$

$$\mathbf{R} = \int_{\Omega} |H_d(e^{j\omega T})|^2 s(e^{j\omega T}) s^H(e^{j\omega T}) d\omega, \quad (5)$$

The function $H_d(e^{j\omega T})$ is the discrete-time equivalent transfer function of the D/A, lowpass filter and A/D in Fig. 3 and $s(e^{j\omega T}) \in C^{K \times 1}$ is given by

$$\left[s(e^{j\omega T}) \right]_k = e^{-j\omega(k-1)T}, k = 1, 2, \dots, K. \quad (6)$$

Note that (2) is quadratic in \mathbf{g} and therefore defines a convex region in K -dimensional space. The least-squares optimisation problem can now be formulated as

$$\min_{\mathbf{g}} [J(\mathbf{g})]. \quad (7)$$

The vector of filter weights, $\check{\mathbf{g}}$, that minimises $J(\mathbf{g})$ in (7) is found from standard optimisation theory to be

$$\check{\mathbf{g}} = \mathbf{R}^{-1} \mathbf{p}. \quad (8)$$

With straightforward manipulation of (4) and (5), the vector $\mathbf{p} \in R^{K \times 1}$ and the matrix $\mathbf{R} \in R^{K \times K}$ can be expressed equivalently in terms of time-domain parameters as follows

$$[\mathbf{p}]_k = \sum_{n=-\infty}^{\infty} d(nT) h_d((n-k+1)T); k = 1, 2, \dots, K, \quad (9)$$

and

$$[\mathbf{R}]_{k,l} = \sum_{n=-\infty}^{\infty} h_d(nT) h_d((n-k+l)T); k, l = 1, 2, \dots, K, \quad (10)$$

where $d(nT)$ is the desired channel impulse response and $h_d(nT)$ is the discrete-time equivalent impulse response of the D/A, lowpass filter and A/D in Fig. 3. From (9) and (10), the elements of \mathbf{p} are values of the cross-correlation between the desired and actual impulse responses and the rows and columns of \mathbf{R} are values of the auto-correlation sequence of the equivalent discrete-time impulse response of the actual analogue filter.

3. FINDING THE OPTIMUM PRE-COMPENSATION FILTER

From (8) the optimum pre-compensation filter can be estimated providing that measurements on the system can be made which give estimates of \mathbf{p} and \mathbf{R} in terms of frequency-domain parameters as in (4) and (5) or in terms of time-domain parameters as in (9) and (10). In the following we propose an approach to estimate \mathbf{p} and \mathbf{R} from time-domain parameters.

From (9) and (10) it can be seen that an estimate of $h_d(nT)$ must be found ($d(nT)$ is known *a-priori*). A well known technique in system identification is to use a pseudorandom binary noise (PRBN) test signal and cross-correlate the input and output to obtain an estimate of the system impulse response [8] as shown in Fig. 4.

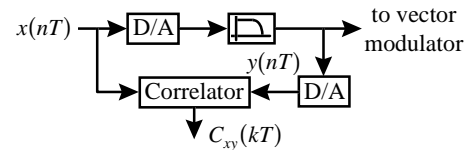


Figure 4. System identification using cross-correlation.

The output of the correlator is given by

$$C_{xy}(kT) = \sum_{l=0}^{L-1} x(lT) y((l+k)T) = h_d(kT) * C_{xx}(kT) \\ \equiv h_d(kT), \quad (11)$$

which is an estimate of the required impulse response of the system. With this estimate, approximate values for \mathbf{p} and \mathbf{R} can

be found from (9) and (10) and an estimate of the optimum pre-compensation filter found from (8).

In practice the A/D converter in Fig 4 is not ideal and quantises the I and Q channel signals into a number of discrete levels. The amplitude quantised signal can be modelled as the original signal, $y(nT)$, plus a quantisation noise, $n_y(nT)$, [10]:

$$y'(nT) = y(nT) + n_y(nT). \quad (12)$$

The output of the correlator therefore becomes

$$C'_{xy'}(kT) = C_{xy}(kT) + C_{xn_y}(kT). \quad (13)$$

For a PRBN input to the filter, $h_d(nT)$, the output (by the Central Limit Theorem) is asymptotically Gaussian. In this situation it can be shown, using an analysis of the characteristic function of the quantiser input [11], that the quantisation noise is uncorrelated with the input signal and $C'_{xy'}(kT)$ is a good estimate of C_{xy} even for coarse quantisation (e.g. total dynamic range divided into 4 levels).

4. SIMULATION STUDIES

4.1 Simulated system configuration

The effectiveness of the proposed digital pre-compensation method is investigated using a computer model of a single channel ERMES (European Radio Message System) modulation format transmitter. The ERMES signal is a 4-PAM (4-level Pulse Amplitude Modulation) CPFSK signal. Pulse shaping of the 4-PAM signal is performed using a 10th order digital Bessel filter before application to the CPFSK modulator. The system sampling frequency is 200 KHz.

Low-pass reconstruction filters, LPF1 and LPF2 in Fig's 1 and 2 have a nominal 6th order Butterworth frequency response with a cut-off frequency of 21.3 KHz. They are implemented using three cascade-connected Sallen & Key 2nd order sections and in the simulation results to follow the circuit component tolerances are assumed to be 5% for resistors and 10% for capacitors. The nominal and actual magnitude and group delay characteristics for LPF1 and LPF2 are shown in Fig. 5.

4.2 System pre-compensation

The FIR pre-compensation filter length is chosen to be 50 taps, ($K = 50$).

It has been found experimentally that departures from a linear-phase characteristic in the reconstruction filters has a significantly more detrimental effect on the output signal envelope than departures from a flat magnitude response in the pass-band of the filters. The magnitude characteristic of the nominal 6th order Butterworth filter is sufficiently flat through the passband and to ensure that degrees of freedom in the optimisation problem are used effectively we set the desired channel response to have the same magnitude characteristic as the nominal magnitude response of the analogue filters but constrain the phase to be linear. Hence, the desired channel response, $D(e^{j\omega T})$, is given by

$$D(e^{j\omega T}, \tau_0) = |H(j\omega)|e^{-j\omega\tau_0}, \quad (14)$$

$$-\omega_s/2 \leq \omega \leq \omega_s/2.$$

where $H(j\omega)$ is the nominal response of the reconstruction filters.

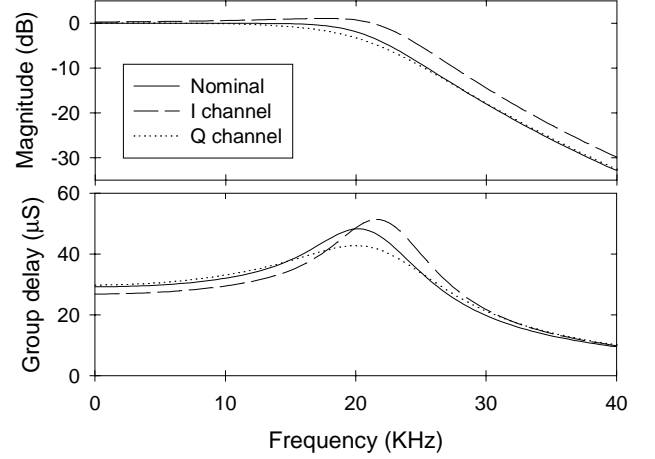


Figure 5. Magnitude group delay responses of the I and Q channel reconstruction filters.

Note that $D(e^{j\omega T}, \tau_0)$ is dependent on the parameter τ_0 which determines the desired system group delay. Since the optimum value of this parameter is not known, the minimisation in (7) must be extended to include it. The optimisation problem can therefore be rewritten as

$$\min_{\tau_0} \left[\min_g [J(g, \tau_0)] \right]. \quad (15)$$

The optimisation over the delay variable, τ_0 , is solved numerically and, for this example, results in an optimum delay value of $\hat{\tau}_0 = 150 \mu\text{S}$.

The PRBN test signal comprises one period of length 16383 samples of a maximal-length shift register sequence [9]. Measurement noise with variance -30dB relative to the square of the peak of the nominal impulse response of the reconstruction filters is added to each channel. The A/D converters are assumed to have an 8-bit quantisation characteristic.

The quantities \mathbf{p} and \mathbf{R} are estimated for each channel and estimates of the optimum I and Q channel pre-compensation FIR filters computed according to (8). The amount of residual AM in the envelope function of the vector modulator output signal is used as a measure of effectiveness of pre-compensation. Fig. 6 shows the envelope functions obtained for the system with and without pre-compensation. These envelope signals were generated using a random sequence of 50 input symbols to the CPFSK modulator.

The nonlinear amplifier shown in Fig. 1 is modelled using a two-parameter formula proposed by Saleh in [3] and used by Pupolin and Greenstien in [2], that closely approximates the amplitude and phase nonlinearities in Travelling Wave Tube (TWT) amplifiers.

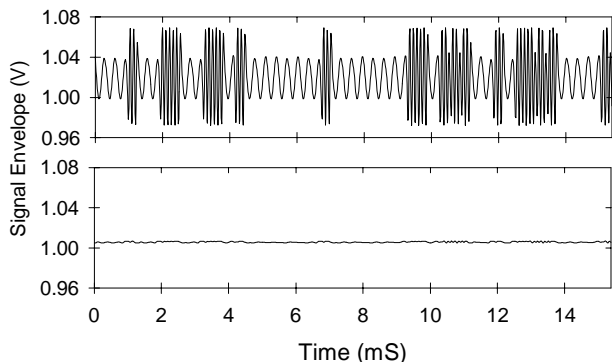


Figure 6. Vector modulator output envelope functions: upper plot: no pre-compensation, lower plot: pre-compensation using PRBN test signals.

Fig. 7 shows the CPFSK signal power spectrum at the output of the amplifier for the system with and without pre-compensation and for a random sequence of 4000 input symbols. The carrier frequency is $f_c = 1$ MHz. Note the increased sidelobes and out-of-band power in the power spectrum for the system with no pre-compensation.

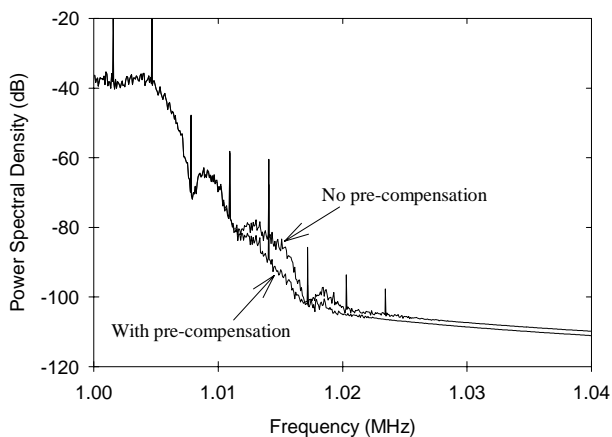


Figure 7. Power amplifier output power spectrum.

The Adjacent Channel Power (ACP) is defined in the ERMES standard as the power in the band from 17 to 33 KHz either side of the carrier. The ACP values computed from the spectrum shown in Fig. 7 are -66 dBc for the system without pre-compensation and -72 dBc for the system with pre-compensation. (The theoretical limit for the signal is -72.1 dBc.) A significant reduction (approximately 6 dBc) in ACP is therefore achieved using the digital pre-compensation method.

5. CONCLUSIONS

The cross-correlation method proposed here allows the optimum digital pre-compensation filters to be estimated using pre-defined PRBN test input signals and provides a means by which automatic pre-compensation can be implemented. As the reconstruction filters characteristics drift relatively slowly with time, "re-training" the FIR pre-compensation filters using the test input signal need only be done at infrequent intervals.

From the extensive numerical studies carried out during the course of this research it appears that maximal-length sequences (or m -sequences) give far superior results in terms of impulse response estimation than other PRBN sequences. This is probably attributable to the fact that m -sequences have the "best" possible autocorrelation function in terms of minimum sidelobe levels for a binary sequence of given period N [9].

Since the pre-compensation technique presented here is not specific to systems generating CPFSK signals, it may also find more general application in IQ modulation systems generating other modulation formats and in equalisation applications.

6. REFERENCES

- [1] S. Haykin, *Communication Systems*, Second Edition, John Wiley & Sons Inc., New York, 1983.
- [2] S. Pupolin and L. J. Greenstein, "Performance Analysis of Digital Radio Links with Nonlinear Transmit Amplifiers," *IEEE Journal on Selected Areas in Comms.*, vol. 5, no. 3, pp. 534-546, April 1987.
- [3] A. A. M. Saleh, "Frequency-Independent and Frequency-Dependent Nonlinear Models of TWT Amplifiers," *IEEE Trans. Comms.*, vol. 29, no 11, pp. 1715-1720, November 1981.
- [4] S. P. Stapleton and F. C. Costescu, "An Adaptive Predistorter for a Power Amplifier Based on Adjacent Channel Emissions," *IEEE Trans. Veh. Tech.*, vol. 41, no. 1, pp. 49-56, February 1992.
- [5] L. Sundstöm, M. Faulkner and M. Johansson, "Effects of Reconstruction Filters in Digital Predistortion Linearizers for RF Power Amplifiers," *IEEE Trans. Veh. Tech.*, vol.44, no.1, pp. 131-138, February 1995.
- [6] S. A. Leyonhjelm and M. Faulkner, "The Effect of Reconstruction Filters on Direct Upconversion in a multichannel Environment," *IEEE Trans. Veh. Tech.*, vol. 44, no. 1, pp. 95-102, February 1995.
- [7] G. C. Goodwin and R. L. Payne, *Dynamic System Identification : experiment design and data analysis*, Academic Press, New York, 1977.
- [8] C. B. Speedy, R. F. Brown and G. C. Goodwin, *Control Theory: Identification and Optimal Control*, Oliver and Boyd, Edinburgh, 1970.
- [9] D. V. Sarwate and M. B. Pursley, "Crosscorrelation Properties of Pseudorandom and Related Sequences," *Proc. IEEE*, vol. 68, no. 5, pp. 593-619, May 1980.
- [10] B. Widrow, "A Study of Rough Amplitude Quantization by Means of Nyquist Sampling Theory," *Trans. IRE*, CT-3, p. 226, 1956.
- [11] D. G. Watts, "A General Theory of Amplitude Quantization with Applications to Correlation Determination," *IEE Monograph*, No. 481M, pp. 209-218, November 1961.